Planet. Space Sci., Vol. 31, No. 2, pp. 221–233, 1983
Printed in Great Britain.

0032–0633/83/020221–13$03.00/0

COMPARISON OF ABSOLUTE PHOTOELECTRON FLUXES MEASURED ON AE-C AND AE-E WITH THEORETICAL FLUXES AND PREDICTED AND MEASURED N_2 2PG 3371Å VOLUME EMISSION RATES

S. P. HERNANDEZ and J. P. DOERING
Department of Chemistry, The Johns Hopkins University, Baltimore, MD 21218, U.S.A.

V. J. ABREU
Space Physics Research Laboratory, University of Michigan, Ann Arbor, MI 48109, U.S.A.

and

G. A. VICTOR
Harvard-Smithsonian Centre for Astrophysics, 60 Garden Street, Cambridge, MA 02138, U.S.A.

(*Received* 26 *July* 1982)

Abstract—As part of the continuing effort to improve the accuracy of the absolute measurements of the ambient photoelectron flux in the thermosphere from the Atmosphere Explorer Satellite Photoelectron Spectrometer experiments (PES), we present a detailed comparison of experimental photoelectron fluxes from AE-C and AE-E together with theoretical calculations of the ambient flux for the same geophysical conditions. As an additional check, the various experimental and theoretical fluxes are used to calculate the expected N_2 2PG (0, 0) volume emission rate expected at 3371Å and these results are compared to AE-C Visible Airglow Experimental (VAE) experimental results. The comparisons clearly show that because of spacecraft shielding of the sensor on AE-C, the agreement with AE-E spectra for similar geophysical conditions ranges from good when shielding is minimal to poor for severe shielding cases. The calculated fluxes are lower by approx. a factor of 1.5–2.0 in absolute magnitude than the AE-E or unshielded AE-C fluxes. The N_2 2PG volume emission rates calculated from the measured ambient electron fluxes overestimate the measured VAE volume emission rates by 20–30% while those calculated from the theoretical fluxes underestimate the measured emission rate by typically 30%. These data suggest therefore that the measured AE-E fluxes are 20–30% high.

INTRODUCTION

Low energy electrons produced at ionospheric altitudes from photoionization of the ambient atomic and molecular species by the solar extreme u.v. flux play an important role in the mechanism by which solar energy is absorbed in the thermosphere. The ambient photoelectron energy distribution in the thermosphere has been the object of extensive measurements and theoretical calculations. Early work has been reviewed by Doering *et al.* (1975). More recently, the Photoelectron Spectrometer Experiments (PES) on Atmosphere Explorer satellites have been making detailed measurements of the ambient photoelectron flux over the entire Earth's surface at all local times. Discrete energy loss calculations of the ambient photoelectron spectrum were first presented by Victor *et al.* (1976a). The results of the experiments and calculations have been discussed by Lee *et al.* (1980a, b) for altitudes from 150 to 1000 km. The general conclusion reached was that the processes involved in the production of the ambient photoelectron spectrum were well understood since excellent agreement was obtained between the shape of the experimentally measured spectrum—especially for the improved measurement on Atmosphere Explorer E—and the theoretical discrete energy loss calculation spectrum. However, although initially encouraging results were obtained for the agreement between the absolute magnitude of the calculated flux and the AE-C satellite measurements, the later, much higher resolution AE-E results were found to be a factor of 2–3 higher than the calculated results over the entire energy range. Calculations by Oran and Strickland (1978), Jasperse and Smith (1978), Richards and Torr (1981), and Richards *et al.* (1982), which use somewhat different cross section data, have produced better absolute agreement with the experimental spectrum.

In the present work, we shall explore the reliability of the Atmosphere Explorer PES measurements of absolute flux by a comparison of the N_2 second positive emission system (0, 0) band intensity measured on AE-C by the Visible Airglow Experiment (VAE) with the intensity calculated from the simultaneously measured PES electron fluxes and N_2 density.

Because of the energy dependence of the N_2 2PG electron impact excitation cross section, the comparison tests the photoelectron spectrum mainly between 12 and 35 eV and is particularly sensitive to the cross section peak region near 14 eV. Kopp *et al.* (1977) have previously used the ambient photoelectron spectrum as calculated by Victor and the measured N_2 density to compare the expected N_2 2PG (0, 0) intensity with their VAE measurements and have obtained reasonable agreement although the calculated emission rate was somewhat lower than what was observed. In this work, we have examined both the AE-C and AE-E results. Unfortunately, there was no VAE experiment on AE-E so the N_2 2PG emission was not measured. However, by judicious choice of AE-E orbital passes which had similar N_2 density and solar zenith angle to previous AE-C passes, it was possible to compare the AE-C and AE-E results. The comparison was greatly facilitated by the low solar activity throughout the 1974–76 period.

The main object of this work was to test the agreement between the measured N_2 2PG emission and that expected on the basis of the photoelectron fluxes and N_2 density to see if a consistent pattern of agreement or disagreement could be found. In addition, we have computed expected N_2 2PG intensities based on new calculations for the ambient photoelectron flux for the actual orbits considered. The comparisons between theory and experiments given in this paper represent a least favorable case as recent calculations based on different cross sections give larger fluxes as mentioned above.

INSTRUMENTATION AND DATA ANALYSIS

Aeronomic data used in this study were obtained from simultaneous measurements of experiments onboard Atmospheric Explorer satellites C and E. Photoelectron fluxes were taken from measurements of the Photoelectron Spectrometer (PES) Experiment (Doering *et al.*, 1973); airglow data were obtained from measurements by the Visible Airglow Experiment (VAE) (Hays *et al.*, 1973); and neutral N_2 density data were taken from measurements by the Open Source Mass Spectrometer (OSS) Experiment (Nier *et al.*, 1973) and the Neutral Atmosphere Composition Experiment (NACE) (Pelz *et al.*, 1973). Since the Visible Airglow Experiment on the AE-E satellite did not measure the thermospheric emission feature at 3371Å only AE-C airglow and neutral composition data were used in this study.

Detailed discussions of the instrumentation and performance of the AE-PES experiments have been given by Doering *et al.* (1973, 1975). In brief, the AE-C and AE-E satellites were launched in December 1973 and November 1975, respectively. Orbital inclination was 68° for the C-spacecraft and 22° for the E-satellite. The PES experiment consisted of two 180° electrostatic electron energy analyzers with an energy bandpass $\Delta E/E = 2.5\%$ mounted on opposite sides of the normally nonsunlit end of the cylindrical spacecraft. When the spacecraft was in a despun mode, the normal sensor position was as follows: sensor 1, on the ram side looking upward (9° off the zenith); sensor 2 on the wake side looking downward (9° off the nadir). For the near equatorial AE-E satellite, sensor 1 (on the ram side) was rotated 90° to look along the spacecraft spin axis (Doering *et al.*, 1976) as shown in Fig. 1. Because of the low latitude coverage of AE-E, the look direction for sensor 1 was always less than 55° from the local geomagnetic field direction and in most cases it was approx. parallel or antiparallel to the magnetic field direction (Doering *et al.*, 1976). It should also be noted that the E sensors produced measurements of higher energy resolution in the 0–32 eV range.

The data set consisted of approx. 90 AE-C and 40 AE-E elliptical orbit passes obtained within the first 3 months of operation of each spacecraft. The altitude range covered was from satellite perigee (140–160 km) to 300 km. Only despun orbital passes were used. Since the data were obtained for early 1974 (for AE-C) and late 1975 and early 1976 (for AE-E) the ambient photoelectron energy distributions measured are representative of the thermosphere under solar minimum conditions. Only sensor 1 data from both spacecraft were used.

Data analysis methods for the airglow data have been presented by Hays *et al.* (1973) and Kopp *et al.*

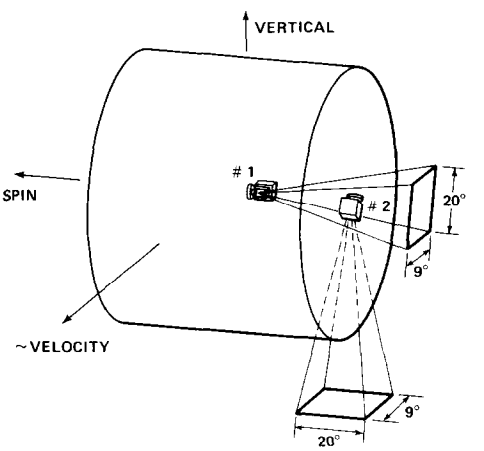

FIG. 1. SCHEMATIC DIAGRAM OF MOUNTING OF PES EXPERIMENT SENSORS 1 AND 2 ON AE-E SPACECRAFT.
Look angles and fields of view are shown. On AE-C and AE-D, the sensor 1 look angle was rotated 90° so that the sensor looked up (antiparallel to sensor 2).

(1977). Analysis of data for AE-C and AE-E PES experiment have been described by Doering *et al.* (1975) and by Lee *et al.* (1980), respectively. The calculations of the equilibrium photoelectron flux in the thermosphere employ the methods of Victor *et al.* (1976a, b) and proceed from a knowledge of solar flux, photoproduction cross sections (Kirby *et al.*, 1979), electron loss cross sections, and neutral particle densities of O, O_2, and N_2. The present calculations were carried out using the data for the specific orbits presented here.

PHOTOELECTRON DATA

Figures 2 and 3 illustrate the present state of agreement between measurements of the ambient photoelectron spectrum from AE-C and AE-E and the calculations. Figure 2 shows the calculated and measured flux for C orbit 677 at an upleg altitude of 222 km. A typical E pass for matching solar zenith angle, neutral densities and altitude is also included. Figure 3 shows the same data for C orbit 677(U) and a similar E pass for 172 km altitude.

The features of the measured ambient photoelectron spectrum have been discussed in detail by Doering *et al.* (1976) and Lee *et al.* (1978). Briefly, the ambient spectrum decreases monotonically to higher energy. A number of important discrete features are observed including the dip near 2.5 eV from the large N_2 resonance inelastic cross section at this energy, the discrete lines between 22 and 28 eV from the

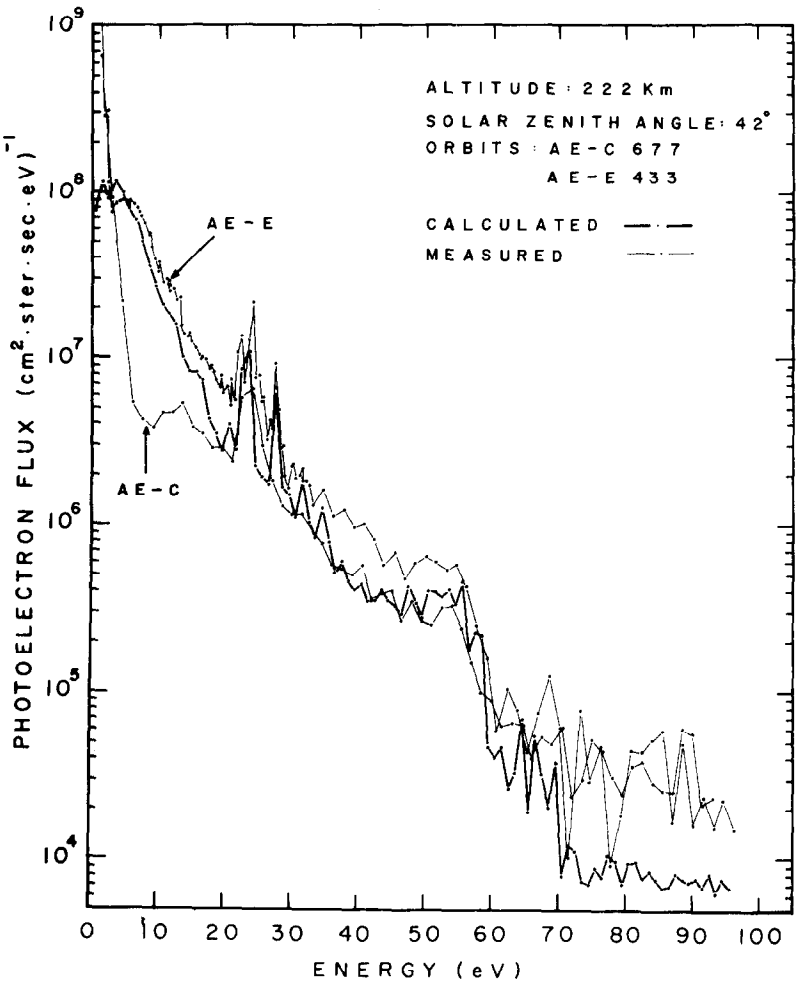

FIG. 2. CALCULATED AND MEASURED AMBIENT PHOTOELECTRON SPECTRA IN THE 0–100 eV RANGE FOR AE-C ORBIT 677(U) AT A MEAN ALTITUDE OF 222 km.

AE-E orbit 433(U) also included has nearly identical solar zenith angle, neutral densities and altitude. Data points from both the 0–32 eV and 0–100 eV sweeps are included in the E pass. Respectively, for the AE-C and AE-E passes: L.T. = 12.0, 10.5, SZA = 42°, 30°, ALT. = 222 km, 221 km.

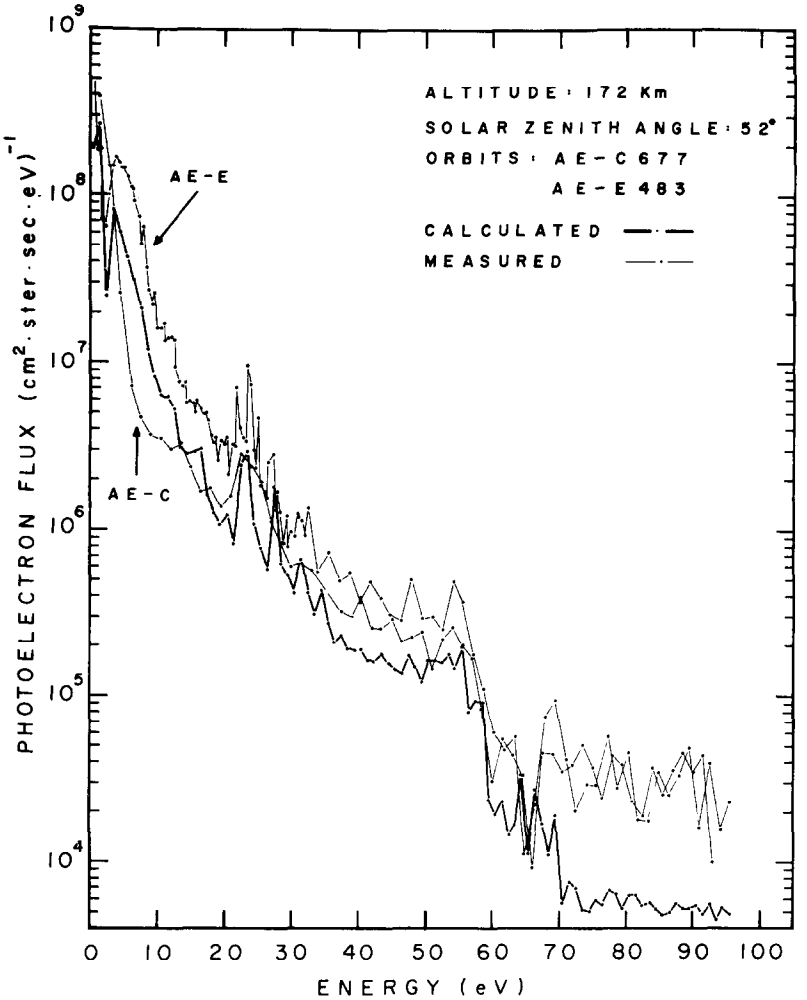

FIG. 3. CALCULATED AND MEASURED AMBIENT PHOTOELECTRON SPECTRA IN THE 0–100 eV RANGE FOR AE-C ORBIT 677(U) AT A MEAN ALTITUDE OF 172 km.
Typical AE-E pass 483(D) matches the C pass in solar zenith angle, neutral densities and altitude. Respectively for the C and E orbits: L.T. = 11.4, 9.0, SZA = 52°, 53°, ALT. = 172 km, 171 km.

photoionization of N_2 and O by the intense solar HeII(304A) line to produce different final electronic states of the ions, and the sharp drop in flux near 60 eV which arises from the relative lack of solar photons having energies greater than 75 eV.

For the 222 km spectra in Fig. 2, the agreement between the calculated flux and the E measurement is better than a factor of 2 over the entire energy range with the E measurements higher than the calculations. Although the absolute agreement between the calculated and measured flux is better above 20 eV for the C measurement than for the E measurement, it can be seen that the C flux drops sharply below 20 eV and there is a large hole near 10 eV. It should also be noted that all measured fluxes above 60 eV are greater than those predicted by the calculations. This effect is simply due to instrument background from the cosmic ray flux, neutral metastable species, and scattered solar photons which cause a small background count rate.

Turning to Fig. 3, it can be seen that at 172 km, the calculated fluxes are lower than the C or E measurements above 20 eV. The measured C flux is intermediate between the calculated flux and the measured E flux. Below 20 eV, however, the C flux again develops a hole and falls below the calculated flux.

In order to understand the differences between the various measured fluxes in Figs. 2 and 3, we must consider the orientation of the sensors with respect to the geomagnetic field. In both cases shown in Figs. 2 and 3, the C sensor 1 was offset slightly from its normal

despun position on the ram side of the spacecraft. However, the geomagnetic field orientation was better from the point of view of spacecraft shielding in the low altitude case. Studies of many C passes of this type have shown that the "hole" in the spectrum between 10 and 20 eV develops when the sensor is "shadowed" by the spacecraft, i.e. when the body of the spacecraft interferes with the spiral electron trajectories in the geomagnetic field. Figure 2 shows a typical case, characteristic of much of the C photoelectron data, where the sensor was in a somewhat unfavorable orientation for the detection of 10–20 eV electrons and a moderate drop in the 10–20 eV flux is produced. In Fig. 3, a case is shown with what we have observed to be the minimum shielding effect for C data. The case shown in Fig. 2 is much more typical and in some cases a much more severe 10–20 eV drop is produced. Data of this type show beyond any doubt that the C photoelectron spectra are all affected to some extent by spacecraft shielding. On the other hand, the E spectra shown in

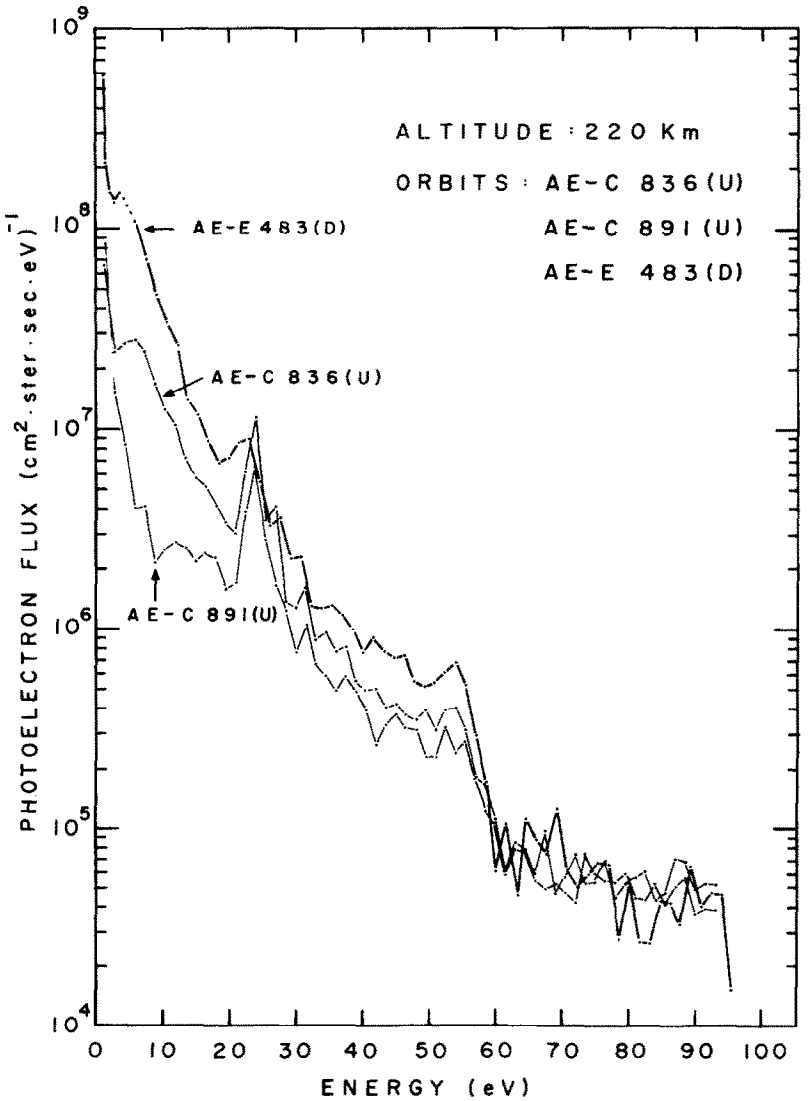

FIG. 4. PHOTOELECTRON SPECTRA IN THE 0–100 eV REGION AT AN ALTITUDE OF 220 km.
From top to bottom: AE-E "normal" despun orbital pass 483(D); AE-C orbit 836(U) taken with sensor in the wake position (rotation of 180° about spacecraft spin axis); AE-C "normal" despun orbit 891(U) with sensor in the ram position. Only data points from the 0–100 eV sweep are included in the E spectrum to facilitate comparison of the spectra. Respectively: L.T. = 8.3, 9.2, 8.3, SZA = 63°, 59°, 66°, ALT. = 223 km; 220 km, 220 km.

Figs. 2 and 3 were taken from normal despun passes and the lack of a drop between 10 and 20 eV and the excellent agreement with the calculated spectral shape shows the dramatic difference produced by the different geomagnetic look direction.

Further conclusions about the influence of spacecraft shielding on the C measurements can be drawn from comparison of the low and high altitude spectra in Figs. 2 and 3 with the calculated flux above 20 eV. In the low altitude case at 172 km where the 10–20 eV shielding is minimal for the C data, the C flux is higher than the calculated flux everywhere above 20 eV. However, for the 220 km data, the measured C flux essentially agrees with the calculated flux. These observations are consistent with an interpretation that the low energy shielding observed in the Fig. 2 data actually extends to much higher energy and that the C spectrum in Fig. 3 at 172 km is higher than the calculation because of reduced shielding.

Further data bearing on these points are presented in Figs. 4 and 5. Figure 4 shows an example of an AE-E spectrum at 220 km and two AE-C spectra at the same altitude and conditions. The AE-E spectrum was obtained in the "normal" E despun orientation. The difference between the two C spectra (taken 5 days apart) was that in one, the C spacecraft was despun but rotated 180° about the spin axis and proceeded through the perigee pass with the sensor in the wake position while the other C pass was in normal orientation. In the C891(upleg) spectrum, the sensor was illuminated by

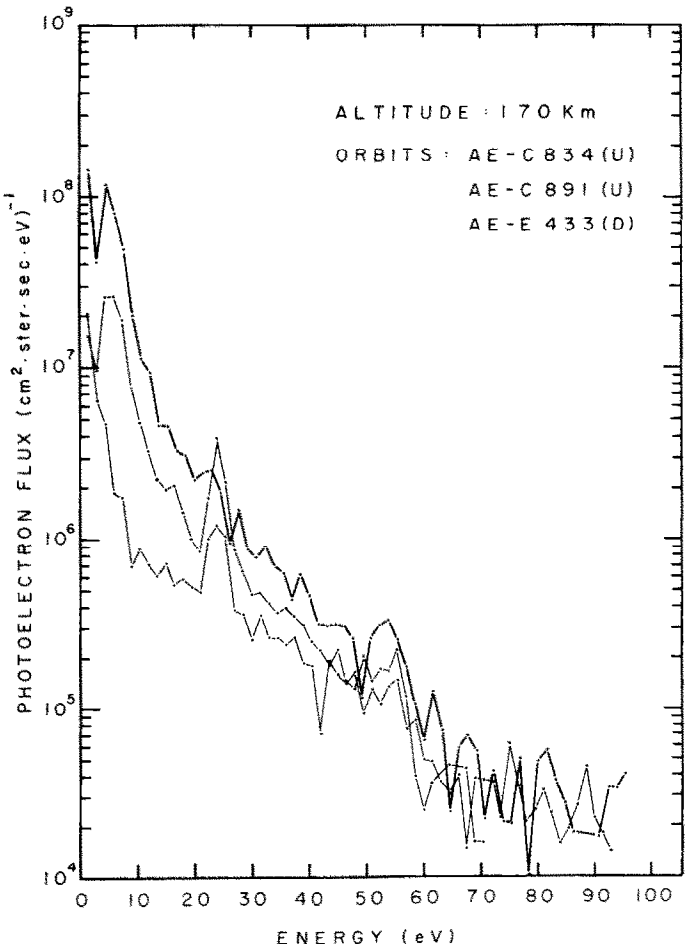

FIG. 5. PHOTOELECTRON SPECTRA IN THE 0–100 eV REGION AT AN ALTITUDE OF 170 km.
From top to bottom: AE-E "normal" despun pass 433(D); AE-C orbit 834(U) taken with sensor in wake position (offset from its normal position by a 180° rotation about spacecraft spin axis); AE-C "normal" despun orbit 891(U) taken with sensor in the ram position. Only data points from the 0–100 eV sweep are included in the E spectrum. Respectively: L.T. = 8.4, 8.8, 7.9, SZA = 67°, 69°, 74°, ALT. = 170 km, 170 km, 170 km.

the sun so a large local spacecraft photoelectron flux appears at the lowest energies as described by Lee *et al.* (1980*a*).

The dramatic differences in the C spectrum produced by the different orientations are obvious in Fig. 4. A large dip appears in the 5–20 eV region of the "normal" C spectrum which is not present in the 180° offset spectrum. In addition, as noted before for the data in Figs. 2 and 3, the offset C spectrum is higher than the "normal" C spectrum over the entire energy range.

A further example of spectra taken with different orientations is shown in Fig. 5. Here data for two C passes and an equivalent E pass taken at 170 km have been plotted for comparison. Note that for these spectra, the sensor was on the shaded side of the spacecraft so the local photoelectron flux was not present (Lee *et al.*, 1980*a*). One C pass, orbit 834(U) was taken with the sensor in the wake and the other (891(U)) with the sensor in the "normal", ram side, position. It can be readily seen again that the "normal" orientation pass shows strong evidence of spacecraft shielding and lies below the other C spectrum over the entire energy range. Although both C spectra are lower in flux than the E spectrum, the 180° "turned around" spectrum is much closer in shape to the E spectrum.

In summary, the data presented in Figs. 2–5 suggest several important points:

(1) Measured C fluxes are always less than measured E fluxes. For cases with favorable geomagnetic sensor altitudes, the spectral shape and magnitude of the C flux agrees best with the E flux.

(2) Spacecraft shadowing of the C sensor is most severe below 20 eV, but some effect persists in severe cases to 60 eV.

(3) Although the calculated fluxes appear to agree well with the >20 eV "normal" C spectra, agreement is poor <20 eV. The measured C fluxes are a factor of 1.5–2 larger than the calculated fluxes for those cases where the effects of shielding below 20 eV on the spectral shape are minimal.

(4) The E spectra agree well in shape with those C spectra where shielding is not important and very well in shape with the calculated fluxes but the E fluxes are approximately a factor of 2 larger than the calculated fluxes.

We are therefore led to conclude that there is a factor of 2 difference between the best measured E photoelectron fluxes and the calculated fluxes. Because of the effects of spacecraft shadowing of the sensor, the C fluxes do not appear to be reliable for determinations of the absolute flux. In view of this discrepancy, it would obviously be extremely desirable to have an independent measurement of the photoelectron flux. Such a measurement is available on AE-C from the Visible Airglow Experiment (VAE) which measured the N_2 2PG (0, 0) band intensity (λ3371 Å). The next section describes the measurement and calculation of the N_2 2PG (0, 0) band volume emission rate.

COMPARISON OF MEASURED AND CALCULATED N_2 2PG VOLUME EMISSION RATE

In this section, we test the measured and calculated photoelectron spectra presented previously by comparing the N_2 2PG (0, 0) band (3371 Å) volume emission rate with the VAE measured values from AE-C. A previous calculation of this type has been carried out by Kopp *et al.* (1977) who found that the volume emission rate predicted from the calculated photoelectron spectrum was somewhat less than the observed rate. In the present study, we shall compare the measured AE-C volume emission rate with rates calculated using

(1) The calculated photoelectron spectrum for specific AE-C passes
(2) The AE-C measured photoelectron spectrum
(3) An AE-E measured spectrum taken under essentially identical conditions of solar zenith angle and N_2 density.

As calculations of this type have been done before (Kopp *et al.*, 1977) only a brief review will be given here. The strong daytime emission feature at 3371 Å is excited solely by direct photoelectron impact on N_2 and cascading processes are negligible. There is also no quenching of the excited state of N_2 ($C^3\Pi_u$) for the total densities of interest here. The excitation cross section and branching ratios for the N_2 2PG are well known (Aarts and DeHeer, 1969; Imami and Borst, 1974). Since the electron impact excitation process involves a spin forbidden singlet-triplet transition, the cross section peaks at a quite low energy (14 eV) and then declines rapidly. An important consequence of the shape of the cross section for the present work is that the electron flux between 12 and 20 eV is primarily responsible for the observed excitation. Figure 6 summarizes the relevant processes, a typical AE-E ambient photoelectron spectrum, and the excitation cross section. Calculation of the excitation rate proceeds in a straightforward manner from the cross section and neutral density data. Figure 7 shows a typical excitation rate ($F \cdot \sigma$) calculation in which the electron flux and cross section have been combined with a point spacing corresponding to the energy interval in the measured electron energy spectrum from AE-E. Two cases are shown for 220 and 172 km. It can be seen that the shape of the excitation rate as a function of energy is dominated by the 12–20 eV region although

the line region between 21 and 26 eV also provides some intensity. These calculations show, therefore, that the N_2 2PG calculated volume emission rate samples mainly the 12–20 eV region of the electron energy spectrum as a consequence of the shape of the cross section.

Once the excitation rate has been calculated, the volume emission rate as a function of altitude can be calculated since:

$$\eta(z) = 4\pi N(z) \int_{E_{th}}^{\infty} F(E, z)\sigma_{3371}(E)\, dE \text{ cm}^{-3}\text{ s}^{-1}$$

where $N(z)$ is the measured N_2 density, E_{th} is the threshold energy (near 11 eV) for the excitation, $F(E, z)$

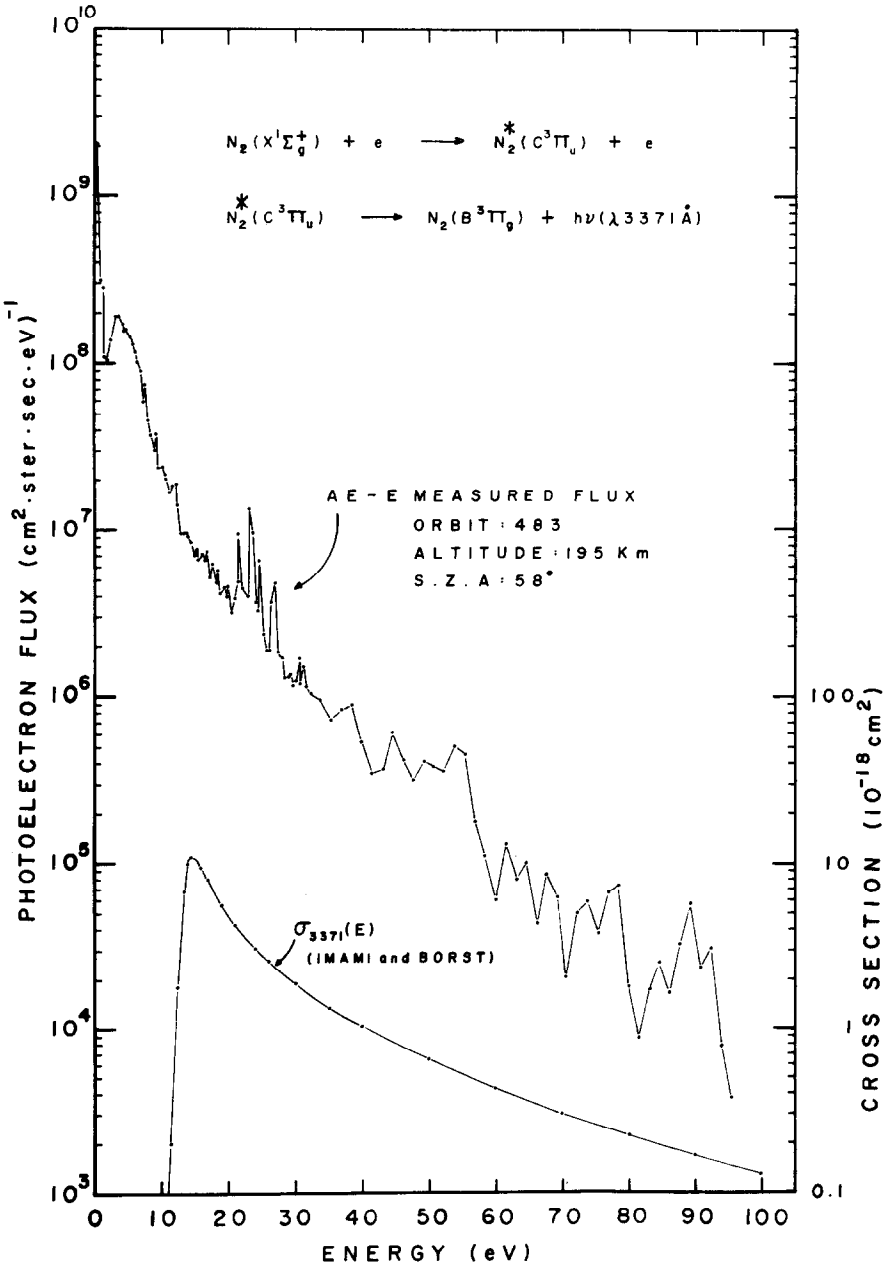

FIG. 6. ENERGY DEPENDENCE OF: (a) PHOTOELECTRON FLUX DISTRIBUTION AT MEAN ALTITUDE OF 195 km AND MEAN SOLAR ZENITH ANGLE OF 58° (L.T. = 8.5) AND (b) THE CROSS SECTION FOR EXCITATION OF THE (0, 0) SECOND POSITIVE BAND AT λ3371Å BY ELECTRON IMPACT.

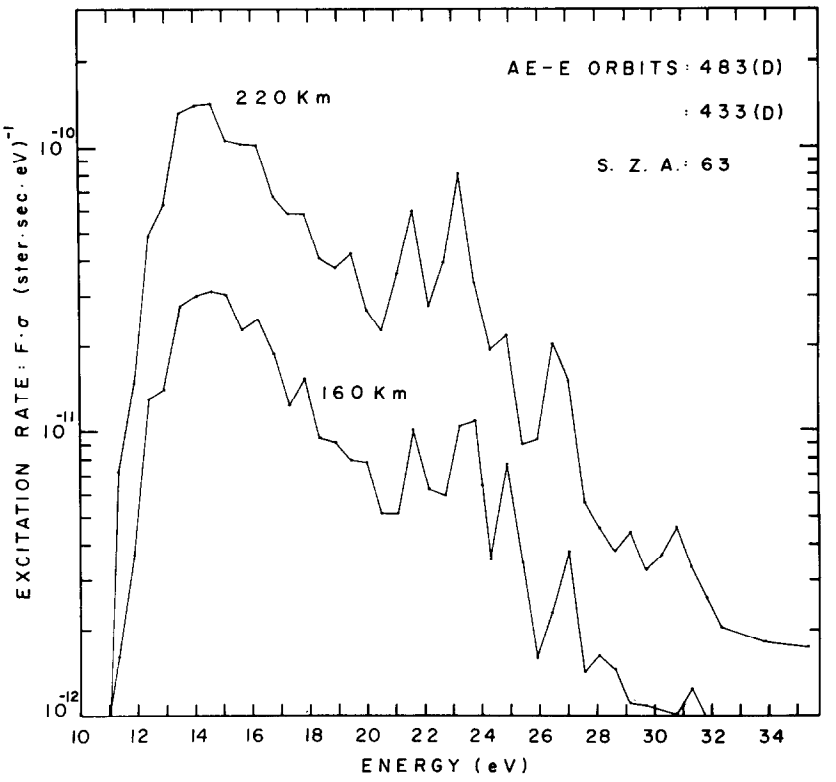

FIG. 7. EXCITATION RATE ($F \cdot \sigma$) PER MOLECULE AS A FUNCTION OF ENERGY AT A SOLAR ZENITH ANGLE OF 63° FOR ALTITUDES OF 220 km (AE-E 433(D)) AND 160 km (AE-E 483(D)).

is the measured or calculated electron flux, and $\sigma_{3371}(E)$ is the N_2 2PG(0,0) band electron excitation cross section. Kopp *et al.* (1977) found that the observed 3371Å volume emission rate for different orbits was strongly dependent on the specific O/N_2 ratio due to the attenuation of the photoelectron flux by atomic oxygen for high values of the ratio. In addition, the volume emission rate increased, as expected, for decreasing solar zenith angles.

The volume emission rate profiles for the 3371Å transition measured by the Visible Airglow Experiment on AE-C are shown in Figs. 8–10. The results of the calculations based on the measured AE-C and AE-E photoelectron flux data are also included. The AE-E calculated volume emission rate profiles were calculated using E fluxes obtained under conditions of altitude, solar zenith angle and neutral composition identical to those for the AE-C data. Volume emission rates using the theoretical photoelectron fluxes are included for some of the orbits. Geophysical data for some of the C orbits analyzed, including the O/N_2 ratio, are given in Table 1. Since the O/N_2 ratio at 170 km was greater than 1.1 for all cases considered, the magnitude of the volume emission rate and its shape vs altitude for each pass was determined mainly by the solar zenith angle variation during the pass. A number of different cases were encountered and the variation of solar zenith angle for each pass is described in the figure captions.

TABLE 1. GEOPHYSICAL DATA FOR SOME OF THE AE-C ORBITS STUDIED AT AN ALTITUDE OF 170 km

AE-C Orbit No.	Date (1974)	Local Time (h)	SZA (deg)	Magnetic latitude	$[O]/[N_2]$	Altitude at η_{max} observed (km)	η_{max} observed (photons $cm^{-3}\ s^{-1}$)
458(U)	Jan. 26	15.4	68°	34° N	1.37	160	19
561(U)	Feb. 5	13.6	54°	30° N	—	~170	30–33
656(U)	Feb. 15	12.0	51°	49° N	1.16	165	39
561(D)	Feb. 5	12.9	65°	49° N	—	160	40
628(D)	Feb. 13	11.7	65°	53° N	1.24	160	28

Neutral density data were not available for all the AE-C passes. In cases where neutral densities were not available, data from the nearest orbital pass (usually within one or two orbits or a few hours) were used.

Figure 8(a) and 8(b) show the measured and calculated volume emission rate profiles for C orbits 656-U and 561-U (U = upleg, D = downleg). The solar zenith angle (SZA) variation was similar for these two orbits and the neutral composition was almost identical. The SZA was approx. 60° at perigee and decreased with increasing altitude. The observed maximum in the volume emission rate in Fig. 8(a) results from the balance between two competing effects: the increase of photoelectron flux and the decrease of the N_2 density with altitude. The differences between the volume emission rates for the two orbits

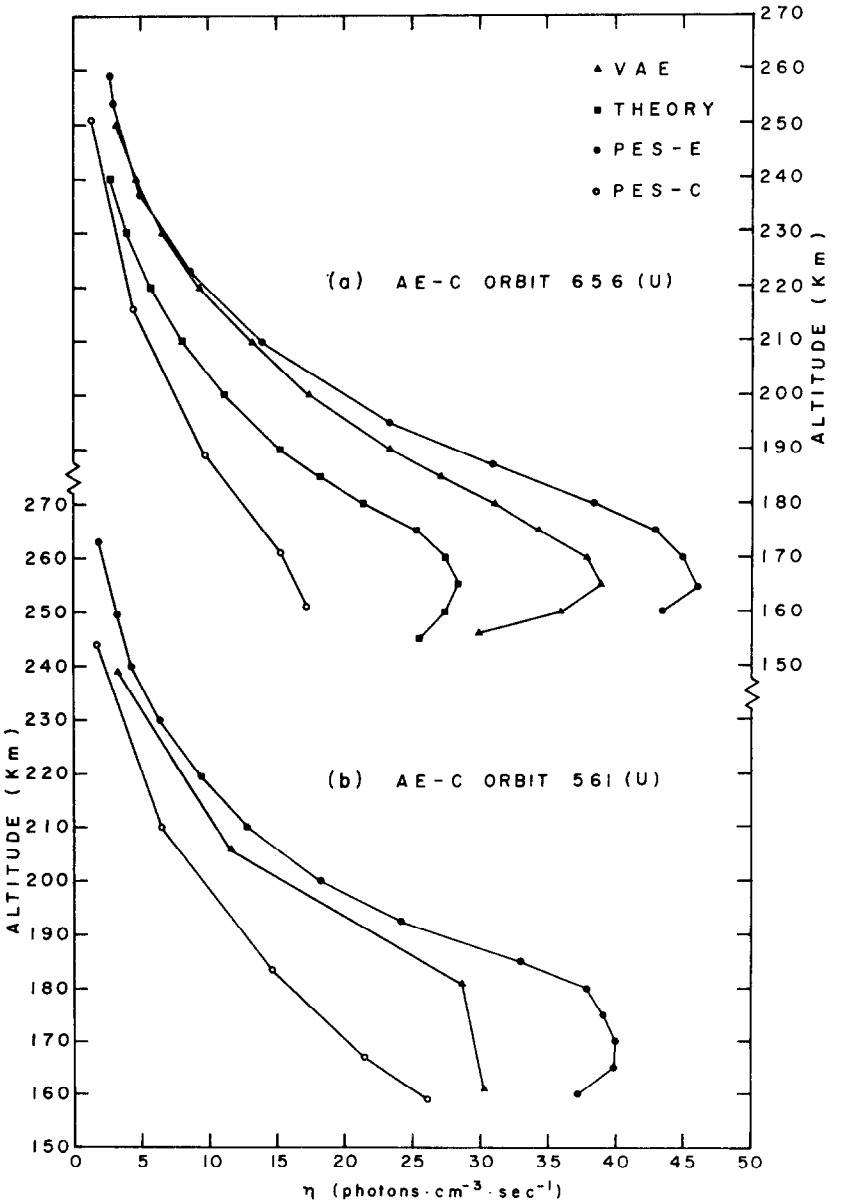

FIG. 8. THE 3371Å MEASURED AND CALCULATED VOLUME EMISSION RATE PROFILES FOR: (a) AE-C ORBIT 556(U) AND (b) AE-C ORBIT 561(U).
Solar zenith angle decreases with increasing altitude from a value of approx. 60° at orbit perigee (155–160 km). PES-E calculation was constructed by averaging 4 to 5 matching AE-E passes at each selected altitude.

are almost entirely due to small SZA differences during the pass.

Figures 9(a) and 9(b) shows the volume emission rates vs altitude for AE-C orbits 628(D) and 561(D). As the SZA dependence was similar to that for Fig. 8, the volume emission rates are similar. Figure 10 shows a case where the SZA was large (~ 70°) near perigee and changed only 4° during the part of the pass shown. The high SZA accounts for the low 3371Å flux and the shift of the peak to higher altitudes (~ 168 km). This result is consistent with the results of Lee *et al.* (1980a) whose work shows that the excitation rate at 160 km is at least 50% lower for a SZA of 70° vs 60°.

Table 2 lists the ratios of the measured volume

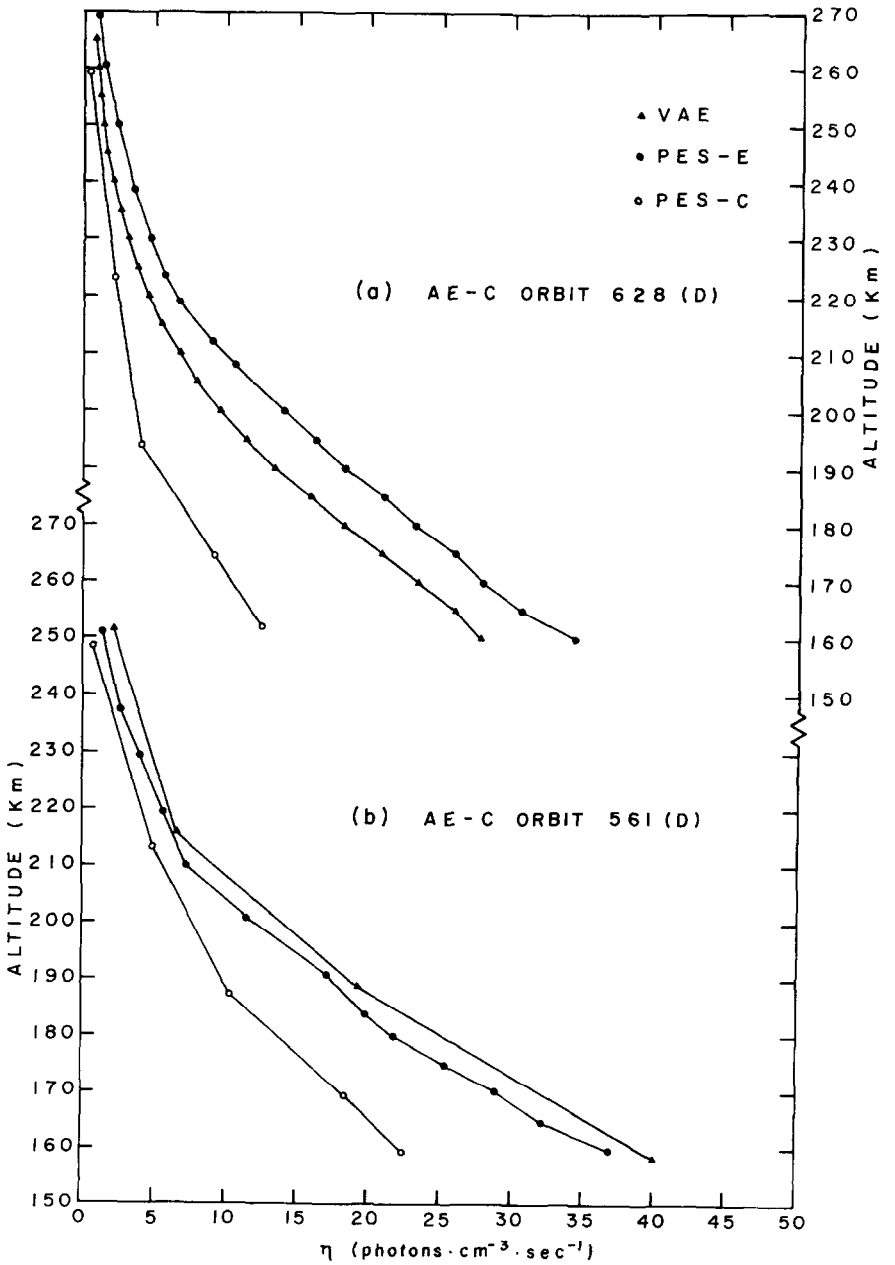

FIG. 9. THE 3371Å MEASURED AND CALCULATED VOLUME EMISSION RATE PROFILES FOR: (a) AE-C ORBIT 628(D) AND (b) AE-C ORBIT 561(D).
Solar zenith angle increases with increasing altitude from approx. 60° at perigee (~ 160 km).

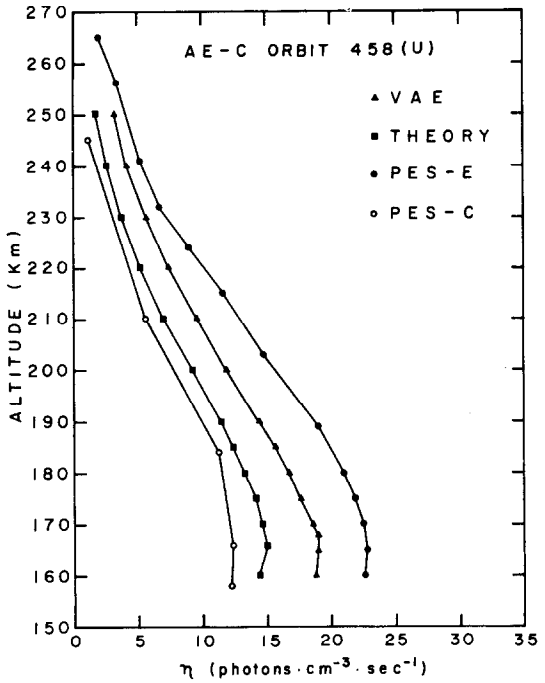

FIG. 10. THE 3371Å MEASURED AND CALCULATED VOLUME EMISSION RATE PROFILES FOR AE-C ORBIT 458(U). Solar zenith angle for this orbit was large (~70° near perigee) and remained essentially constant during the pass (66° at 260 km).

emission rates to the results of the various calculations at 170 and 220 km. In general, the results derived from the calculated photoelectron fluxes are very consistent and account for 70–75% of the observed intensity. The results derived from the AE-C fluxes are highly variable, as expected, because of the different effects of spacecraft shielding in the various passes. For the "offset" passes, the agreement is better than for the "normal" sensor orientation passes; but the agreement varies with altitude as a consequence of the changing geomagnetic attitude of the sensor through the pass. The less shielded C passes predict a maximum of 70% of the observed intensity.

On the other hand, the agreement between the volume emission rates calculated using the AE-E spectrum for identical conditions as the AE-C 3371Å emission rate data is remarkably consistent. The "AE-E" calculations overestimate the volume emission rates by as much as 30% (typically 20–25%) except for orbit 561(D) where 90% of the observed intensity is predicted over the entire altitude range. The AE-E results are quite consistent as would be expected from the lack of magnetic shielding effects in the spectrum.

TABLE 2. RATIOS OF MEASURED VOLUME EMISSION RATES TO THE RESULTS OF THE VARIOUS CALCULATIONS

Orbit	VAE/PES-C	VAE/PES-E	VAE/Theory
(a) Altitude: 170 km			
458(U)	1.54	0.83	1.27
561(U)	1.44	0.74	
656(U)	2.44	0.84	1.38
561(D)	1.78	1.11	
628(D)	2.31	0.84	
(b) Altitude: 220 km			
458(U)	1.85	0.75	1.42
561(U)	1.60	0.86	
656(U)	2.14	0.94	1.62
561(D)	1.46	1.10	
628(D)	1.92	0.72	

CONCLUSIONS

There are several conclusions which can be drawn from the data presented here. First, we have shown that there is a consistent relationship between the ambient photoelectron energy spectra measured on AE-C and those measured on AE-E. Briefly stated, the relationship is that the AE-E spectra provide an upper limit for the AE-C cases. Absolute agreement between the two sets of data varies from good for those cases when spacecraft shielding of the C fluxes is small to poor for severely shielded cases. Agreement between the two sets of fluxes is best for those cases in which the shape of the spectra most nearly agree.

The second conclusion is that the calculated fluxes used here are approximately a factor of two less in absolute magnitude than the AE-E fluxes although agreement between the calculated and observed relative shape of the spectra is excellent. We conclude that comparisons of the calculated and AE-C measured fluxes are not useful because of the variation in AE-C fluxes caused by magnetic shielding. However, we note that the best AE-C spectra where shielding effects are a minimum have absolute intensities a factor of ~1.5 higher than the calculated fluxes in the region above 20 eV where shielding is minimal.

Third, the comparison of the 3371Å N_2 2PG volume emission rate measurements with the volume emission rates calculated from theoretical fluxes, AE-C fluxes, and AE-E fluxes shows that the measured volume emission rates are intermediate in intensity between those calculated from the theoretical flux and those calculated from the AE-E flux. Results for calculations using the AE-C fluxes are, as expected, highly variable.

The data in Table 2 show that calculations using the theoretical fluxes underestimate the N_2 2PG emission rate by 30% and those using the AE-E fluxes overestimate the emission rate by 20–30%. We conclude, therefore, that over the region tested by the

comparison AE-E fluxes are probably high by 20–30%; but within the original ±30% uncertainty of the original measurement.

Acknowledgements—This work was supported by the National Aeronautics and Space Administration under contracts NAS5-11415, NAS5-11437, and NAS5-23006. The authors wish to acknowledge the helpful discussions with Dr. J. S. Lee. M. Whealton provided valuable assistance in the preparation of the illustrations.

REFERENCES

Aarts, J. F. M. and DeHeer, F. J. (1969) Emission cross sections of the second positive group of nitrogen produced by electron impact. *Chem. Phys. Lett.* **4**, 116.

Doering, J. P., Bostrom, C. O. and Armstrong, J. C. (1973) The photoelectron spectrometer experiment on Atmosphere Explorer. *Radio Sci.* **8**, 387.

Doering, J. P., Peterson, W. K., Bostrom, C. O. and Armstrong, J. C. (1975) Measurement of low-energy electrons in the day airglow and dayside auroral zone from Atmosphere Explorer-C. *J. geophys. Res.* **80**, 3934.

Doering, J. P., Peterson, W. K., Bostrom, C. O. and Potemra, T. A. (1976) High resolution daytime photoelectron energy spectra from AE-E. *Geophys. Res. Lett.* **3**, 129.

Hays, P. B., Carignan, G. R., Kennedy, B. C., Shepherd, G. G. and Walker, J. C. G. (1973) The visible airglow experiment on Atmosphere Explorer. *Radio Sci.* **8**, 369.

Imami, M. and Borst, W. L. (1974) Electron excitation of the (0, 0) second positive band of nitrogen from threshold to 1000 eV. *J. Chem. Phys.* **61**, 1115.

Jasperse, J. J. and Smith, E. R. (1978) The photoelectron flux in the earth's ionosphere at energies in the vicinity of photoionization peaks. *Geophys. Res. Lett.* **5**, 843.

Kirby, K. K., Constantinides, E. R., Babcu, S., Oppenheimer, M. and Victor, G. A. (1979) Photoionization and photo absorption cross sections of He, O, N_2 and D_2 for aeronomic calculations. *Atomic Data Nuclear Data Tables* **23**, 63.

Kopp, J. P., Rusch, D. W., Roble, R. G., Victor, G. A. and Hays, P. B. Photo-emission in the second positive system of molecular nitrogen in the earth's dayglow. *J. geophys. Res.* **82**, 555, 1977.

Lee, J. S., Doering, J. P., Bostrom, C. O. and Potemra, T. A. (1978) Measurement of the daytime photoelectron energy distribution from AE-E with improved energy resolution. *Geophys. Res. Lett.* **5**, 581.

Lee, J. S., Doering, J. P., Potemra, T. A. and Brace, L. H. (1980*a*) Measurements of the ambient photoelectron spectrum from Atmosphere Explorer: I. AE-E measurements below 300 km during solar minimum conditions. *Planet. Space Sci.* **28**, 947.

Lee, J. S., Doering, J. P., Potemra, T. A. and Brace, L. H. (1980*b*) Measurements of the ambient photoelectron spectrum from Atmosphere Explorer: II. AE-E measurements from 300 to 1000 km during solar minimum conditions. *Planet. Space Sci.* **28**, 973.

Nier, A. O., Potter, W. E., Hickman, D. R. and Mauersberger, K. (1973) The open-source neutral-mass spectrometer on Atmosphere Explorer-C, -D, and -E. *Radio Sci.* **8**, 271.

Oran, E. S. and Strickland, D. J. (1978) Photoelectron flux in the Earth's atmosphere. *Planet. Space Sci.* **26**, 1161.

Pelz, D. T., Reber, C. A. and Hedin, A. E. (1973) A neutral-composition experiment for the Atmosphere Explorer-C, -D, and -E. *Radio Sci.* **8**, 277.

Richards, P. G. and Torr, D. G. (1981) A formula for calculating theoretical photoelectron fluxes resulting from the He^+ 304Å solar spectral line. *Geophys. Res. Lett.* **8**, 995.

Richards, P. G., Torr, D. G. and Espy, P. J. (1982) Determination of photoionization branching ratios and total photoionization cross sections at 304Å from experimental ionospheric photoelectron fluxes. *J. geophys. Res.* **87**, 3599.

Victor, G. A., Kirby-Docken, K. and Dalgarno, A. (1976a) Calculations of the equilibrium photoelectron flux in the thermosphere. *Planet. Space Sci.* **24**, 679.

Victor, G. A., Kirby-Docken, K. and Dalgarno, A. (1976b) The equilibrium photoelectron flux in the thermosphere. *EOS* **57**, 298.